Synthesis and structural characterization of phosphate-based Nasiglasses Na$_3$Ca$_{1-x}$Mn$_x$Ti(PO$_4$)$_3$ (0 ≤ x ≤ 1(

S. Lamrhari [1], Z. El Khalidi [1], S. Krimi [2], M. Haddad [3], M. Couzi [4], A. Lachgar [5], A. El Jazouli [1*]

[1]*LCMS/LCPCE-URAC17, Faculté des Sciences Ben M'Sik, Université Hassan II, Casablanca, Morocco.*
[2]*LPCMI, Faculté des Sciences Ain Chock, Université Hassan II, Casablanca, Morocco.*
[3]*LASMAR-URAC11, Faculté des Sciences, Université Moulay Ismaïl, Meknès, Morocco.*
[4]*Université de Bordeaux, CNRS, ISM UMR 5255, 351 cours de la Libération, F-33405 Talence Cedex, France.*
[5]*Department of Chemistry, Wake Forest University, Winston-Salem, North Carolina, USA.*

Abstract

Nasiglasses with formula Na$_3$Ca$_{1-x}$Mn$_x$Ti(PO$_4$)$_3$ (0 ≤ x ≤ 1) were synthesized and structurally characterized by DTA, PXRD, EPR, Raman, and density measurements. The density of these glasses increases while the molar volume remains practically constant when manganese replaces calcium, indicating that manganese ions are located in the interstitial sites of the framework, in good agreement with the small variation of the glass transition temperature, observed between the extreme compositions ($\Delta T_g = 23$ °C). Crystallization of the glasses at 650 °C leads to the formation of crystalline phases belonging to the Nasicon family. The structure of these crystalline phases consists of three dimensional framework built of PO$_4$ tetrahedra sharing corners with AO$_6$ octahedra (A = Ca/Mn, Ti); Na$^+$ ions occupy the interstitial sites. EPR study of glasses shows that Mn^{2+} ions occupy octahedral sites, with predominantly ionic bonding between Mn^{2+} and O^{-2} ions. Raman spectroscopy study shows that the glasses contain P$_2$O$_7$ and PO$_4$ groups, and short -Ti-O-Ti-O-Ti- chains. The presence of these chains indicates that the TiO$_6$ octahedra are linked to each other through corners, unlike in the corresponding crystalline phases where they are connected to each-other via PO$_4$ tetrahedra. All results obtained for the glassy materials indicate that Mn^{2+} and Ca^{2+} ions act as glass modifiers, unlike in the crystalline compounds where they are part of the framework.

1. Introduction

Metal phosphates in both crystalline and glassy forms are extensively studied for their potential applications. They can be used as hosts for radioactive elements which makes them useful in removal of radioactive elements from nuclear waste [1,2], as cathodes in lithium ion batteries [3,4], as sunscreens for UV radiation absorption [5,6], as pigments [7-10], as lasers and light emitting diodes (LEDs) components [11,16], and last but not least as biomaterials [17,22]. Phosphate glasses possess a series of interesting properties such as low glass transition temperatures, low melting and softening temperatures, high electrical conductivity and interesting dielectric properties [23], large thermal expansion coefficients [24], and high optical transparency window over UV, visible and infrared wavelength range [25]. Introduction of divalent manganese ions (Mn^{2+}) in phosphates leads to materials with interesting electrochemical, optical, thermochemical, and electric-dielectric properties [3,14, 26-28]. The diverse properties and applications of phosphate glasses depend on their structure, which is based on the distribution of PO$_4$ tetrahedra in the vitreous network. Connection of these tetrahedra by vertices gives rise to different phosphate groups depending on the value of O/P ratio. So, the glass structure can be formed by

a cross-linked network where each PO_4 is linked to three others (vitreous P_2O_5, O/P = 2.5), infinite metaphosphate chains where each PO_4 is linked to tow others (vitreous $NaPO_3$, O/P = 3), or by small diphosphate $P_2O_7^{2-}$ (O/P = 3.5) and monophosphate PO_4^{3-} (O/P = 4) anions [29]. We previously reported the study of glasses belonging to the Na_2O-TiO_2-P_2O_5 system [30]. This ternary system includes the composition $Na_5Ti(PO_4)_3$ (50 mol. % Na_2O - 20 mol. % TiO_2 - 30 mol. % P_2O_5), which exists in both glassy and crystalline forms [31, 32]. The crystalline form belongs to the Nasicon family (Nasicon is the acronym of Natrium super ionic conductor) [33, 34]. Many compounds of this family can be prepared in the glassy form; they are called Nasiglass (Na super ionic glass) [35]. Substitution of sodium in $Na_5Ti(PO_4)_3$ by calcium or manganese led to formation of new crystalline and vitreous compounds $Na_{5-2x}Ca_xTi(PO_4)_3$ ($0 \leq x \leq 1$) [36, 37] and $Na_{5-2x}Mn_xTi(PO_4)_3$ ($0 \leq x \leq 1$) [38]. The composition x = 1 corresponds to the compounds $Na_3CaTi(PO_4)_3$ and $Na_3MnTi(PO_4)_3$. The structure of their crystalline form consists of a three dimensional framework built of PO_4 tetrahedra sharing corners with AO_6 octahedra (A = Ca/Mn, Ti); Na^+ ions occupy interstitial sites. Ti^{4+}, Ca^{2+}, and Mn^{2+} ions belong to the framework of these crystalline materials [39-41]. Raman study of glassy form of $Na_3CaTi(PO_4)_3$ showed the presence of short -Ti-O-Ti-O-Ti- chains [37]. In order to have more information on the structure of the glass, we substituted manganese for calcium and used Mn^{2+} ion as paramagnetic local probe. The present paper reports the synthesis and structural characterization of $Na_3Ca_{1-x}Mn_xTi(PO_4)_3$ ($0 \leq x \leq 1$) system (30 mol. % Na_2O – 20(1-x) mol. % CaO – 20x mol. % MnO – 20 mol. % TiO_2 – 30 mol. % P_2O_5; $0 \leq x \leq 1$).

2. Experimental details

Glassy samples of $Na_3Ca_{1-x}Mn_xTi(PO_4)_3$, $0 \leq x \leq 1$, were prepared by the conventional melt-quenching technique, using analytical grade reagents NaH_2PO_4, $CaCO_3$, TiO_2 and MnO. Before weighing the reagents, $CaCO_3$ is dried at 350°C and TiO_2 at 600°C, during 4 hours, in order to remove any traces of water and adsorbed gases, then kept in dry atmosphere. The overall chemical reaction is summarized in the following equation:

$$3NaH_2PO_4 + (1-x)CaCO_3 + xMnO + TiO_2 \longrightarrow Na_3Ca_{1-x}Mn_xTi(PO_4)_3 + 3H_2O + (1-x)CO_2$$
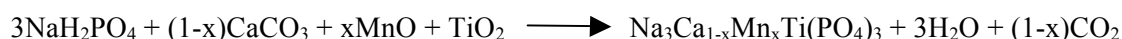
Stoichiometric amounts of reagents, required to obtain 10g of the glass, were ground in a porcelain mortar then transferred to a platinum crucible. The mixture was heated at 200°C (4h) and 600°C (6h) to eliminate H_2O and CO_2 gases. The temperature was then progressively raised to 1050°C with a heating rate of 10 °C/min, and held for 20 min at this temperature. The melt was then quenched to room temperature in air. Homogeneous glasses without bulbs were obtained. $Na_3CaTi(PO_4)_3$ is colorless while glasses containing manganese are brown (Figure 1). The brown color becomes more intense when the manganese content increases. Crystallization of glasses consists of heating powders of the previously prepared samples for 12 hours at 650°C (temperature close to the crystallization temperature T_c of the glasses). Crystalline form of $Na_3CaTi(PO_4)_3$ has a white color, while the compounds containing manganese have a brownish color as seen in Figure 1.

Glassy samples							
Crystalline samples							
x	**0**	**0.01**	**0.05**	**0.25**	**0.50**	**0.75**	**1**
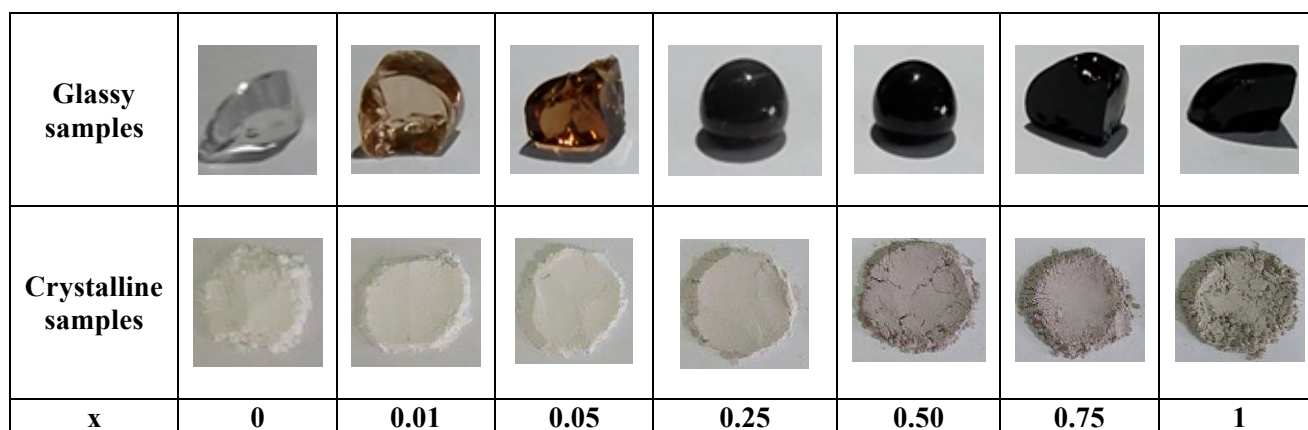
Figure 1: Photographs of glassy and crystalline $Na_3Ca_{1-x}Mn_xTi(PO_4)_3$ ($0 \leq x \leq 1$) samples.

Density measurements were performed on blocks of glasses, using Archimedes' Principle, on an analytical balance (±0.1 mg) with an attached density kit. Diethyl phthalate was used as the immersion liquid. The density (ρ) was obtained from the following equation:

$$\rho = [m_a/(m_a-m_l)] \, \rho_l$$

where m_a is the mass of the sample in air, m_l is the mass of the sample fully immersed in the liquid, and ρ_l is the density of liquid used (diethyl phthalate) at room temperature. Measurements were done three times for each composition, and the error is within ± 0.03 g/cm³. The molar volume ($V_m = M/\rho$) of glasses was calculated from the molecular weight (M) and density (ρ).

Differential scanning calorimetry (DSC Q2000, heating rate 10 °C/min, accuracy ±5°C) was used to determine the glass transition and crystallization temperatures of the glasses (T_g, T_c). Crushed glass powders (~20 to 40 mg) were transferred to platinum crucibles and the curves were recorded in air atmosphere.

Powder X-ray diffraction (PXRD) patterns were recorded at room temperature with a powder diffractometer (PANalytical X'Pert Pro) using Cu K_α radiation (1.54 Å).

Raman spectra were recorded on small pieces of glasses, on a confocal micro-Raman Labram (Horiba/Jobin-Yvon) spectrophotometer with a backscattering mode, at room temperature, in the range 150-1800 cm⁻¹. The excitation source was a 532 nm continuous laser. A holographic Notch filter was used to reject the Rayleigh diffusion. The backscattered light was collected through a 100x objective and selectively transmitted toward a cooled CCD detector. EPR spectra were recorded at room temperature with a Bruker spectrometer operating at the X-band frequency (9.7 GHz).

3. Results and discussion

3.1. PXRD of glasses

The amorphous state of glasses was checked by PXRD. The absence of any sharp peak in the diffraction patterns of $Na_3Ca_{1-x}Mn_xTi(PO_4)_3$ ($0 \leq x \leq 1$) glasses (Figure 2) confirms their amorphous state.
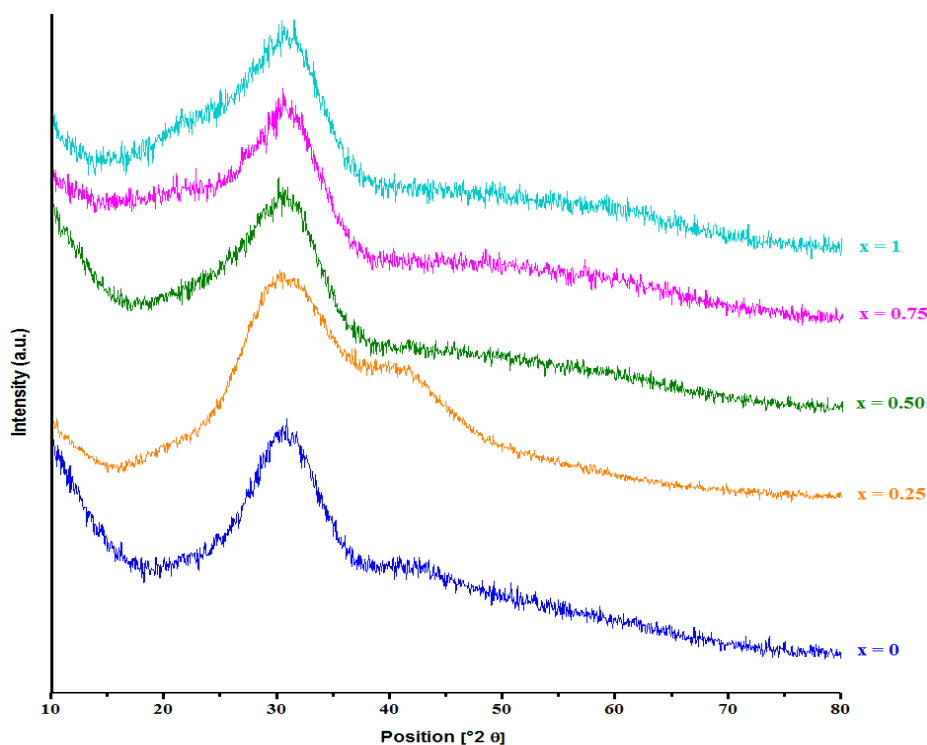
Figure 2: PXRD patterns of glassy $Na_3Ca_{1-x}Mn_xTi(PO_4)_3$ ($0 \leq x \leq 1$)

3.2. Density and molar volume

The density and molar volume of glasses depend upon many factors such as structure, coordination number, cross-link density, and dimensionality of interstitial spaces [42]. If the molar volume remains constant, we can conclude that the cations introduced are located in the interstitial sites of the framework. A decrease in the molar volume shows that the introduced cations occupy sites available within the framework, and strengthens the network as it bridges the oxide ions. An increase in molar volume is indicative of a network expansion. The values of molar mass ($M = 0.3\ M_{Na2O} + 0.2(1-x)\ M_{CaO} + 0.2x\ M_{MnO} + 0.2\ M_{TiO2} + 0.3 M_{P2O5}$; $0 \leq x \leq 1$), density (ρ) and molar volume (V_m) for the studied glasses are reported in table 1. With an increase in MnO content, the molar weight and the density increase while the molar volume remains practically constant, within the accuracy of the measurements. The increase of the molar mass and the density is due to replacement of low molecular weight Ca^{2+} by Mn^{2+}. The fact that the molar volume remains practically constant, when MnO concentration

increases, indicates that Mn^{2+} ions occupy the interstitial sites, and don't participate to the glass framework. Thus, one can conclude that MnO acts as glass modifier.

3.3. DSC study

DSC thermograms of the glasses studied are shown in Figure 3. All glasses exhibit an endothermic change due to glass transition, followed by an exothermic peak due to crystallization of the glass. Data in Table 1 show that the values of the glass transition temperature (T_g) and crystallization temperature (T_c) decrease with increasing MnO content. However the variation of T_g between the extreme compositions ($\Delta T_g = 23 \pm 10°C$) is not as important as those observed in Na_2O-MnO-P_2O_5 ($\Delta T_g = 120°C$) and K_2O-MnO-P_2O_5 ($\Delta T_g = 185°C$) glasses [27, 43]. It is established that the variation of glass transition temperature is strictly related to the nature of bonding in the vitreous network. A large variation of T_g shows a strong modification of the glass structure. The small variation of T_g observed for $Na_3Ca_{1-x}Mn_xTi(PO_4)_3$ ($0 \leq x \leq 1$) glasses indicates that non significant change occurred in their structure. This behavior is due to the fact that, Mn^{2+} ions are located in the interstitial sites, and don't participate to the glass framework, in good agreement with the non-variation of the molar volume of these glasses.

Table 1. Density (ρ), molar mass (M), molar volume (V_m), glass transition temperature (T_g) and crystallization temperature (T_c) of $Na_3Ca_{(1-x)}Mn_xTi(PO_4)_3$ ($0 \leq x \leq 1$) glasses.

x	ρ (g/cm³ 0.03 ±)	M (g/mol)	V_m (cm³/mol 0.4 ±)	T_g (C° 5 ±)	T_c (C° 5 ±)
0	2.85	88.37	31.0	498	609
0.25	2.89	89.11	31.1	487	596
0.50	2.90	89.85	31.0	480	601
0.75	2.95	90.59	31.0	479	608
1	3.02	91.34	31.0	475	576
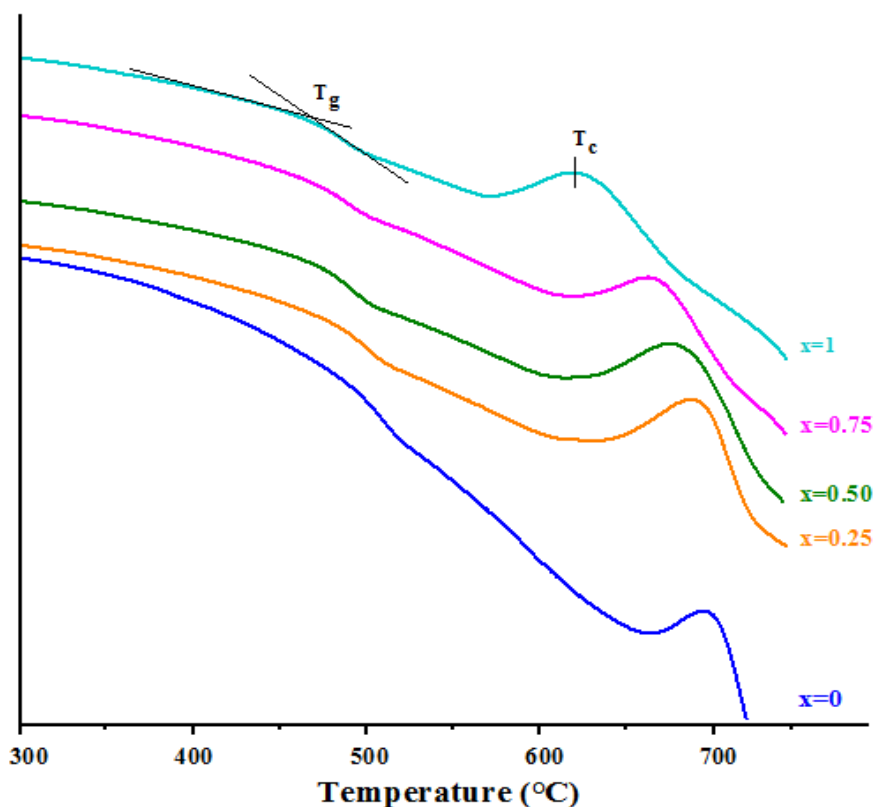
Figure 3: DSC curves of $Na_3Ca_{1-x}Mn_xTi(PO_4)_3$ ($0 \leq x \leq 1$) glasses.

3.4. Powder X-ray diffraction of the crystalline materials

The PXRD patterns of the crystalline $Na_3Ca_{1-x}Mn_xTi(PO_4)_3$ materials, obtained by crystallization of the glasses at 650°C, are shown in Figure 4, for the compositions $x = 0$ and 1, as examples. They can be indexed in the trigonal system, space group R32. The values of the equivalent hexagonal cell parameters ($a_h = 8.961$ Å; $c_h = 21.929$ Å for $x = 0$ and $a_h = 8.813$ Å; $c_h = 21.748$ Å for $x = 1$) are consistent with the Nasicon-type structure [33, 34]. The very low intensity extra peaks are attributed to $NaTi_2(PO_4)_3$ and $Ca_2P_2O_7$. These impurities are probably due to a low weight loss during the synthesis of glasses at high temperature, implying a slight deviation from the theoretical composition. Details of the crystalline structure of $Na_3Ca_{(1-x)}Mn_xTi(PO_4)_3$ compositions will be described elsewhere. It consists of a 3D network of PO_4 tetrahedra and AO_6 (A = Ti, Ca/Mn) octahedra sharing corners (Figure 5). Within this covalent framework exist two additional cationic sites, usually labeled M1 and M2, where the sodium ions are located. The M1 site is a trigonal antiprism sharing faces with two AO_6 octahedra. The M2 site is a large cage bounded by 8 oxygens. The decrease of the cell parameters when manganese replaces calcium in the octahedral sites can be explained by the size of Mn^{2+} (0.82 Å), which is smaller than that of Ca^{2+} (1.00 Å).
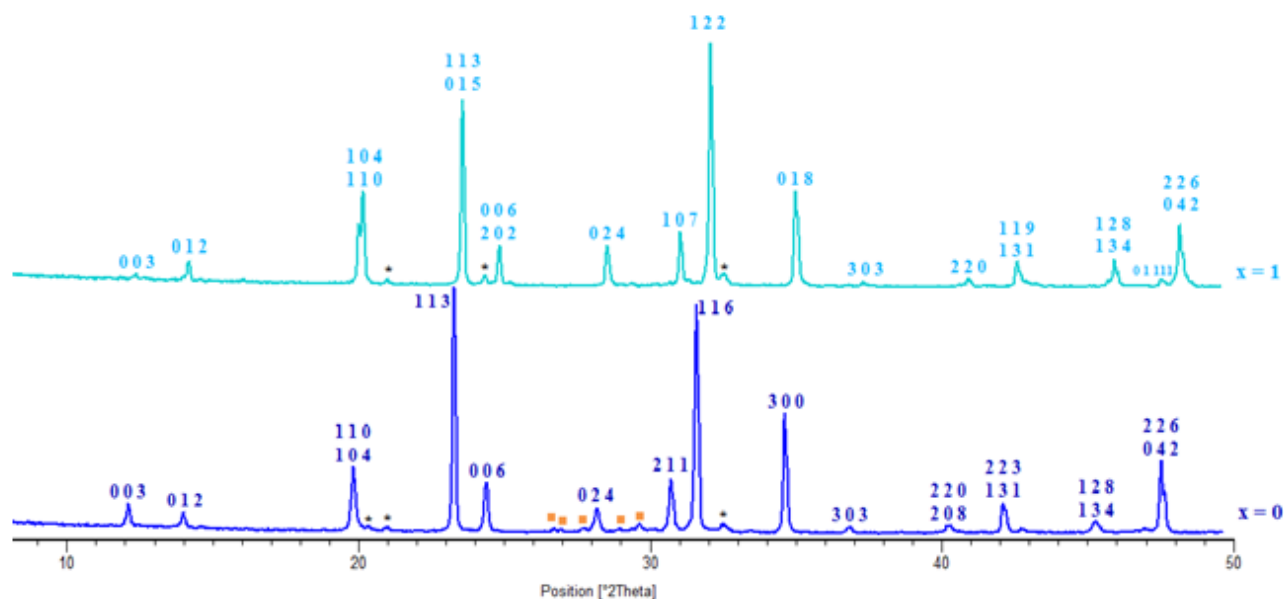
Figure 4: PXRD patterns of crystalline $Na_3Ca_{1-x}Mn_xTi(PO_4)_3$ ($x = 0, 1$) (*: $NaTi_2(PO_4)_3$; ■: $Ca_2P_2O_7$.(
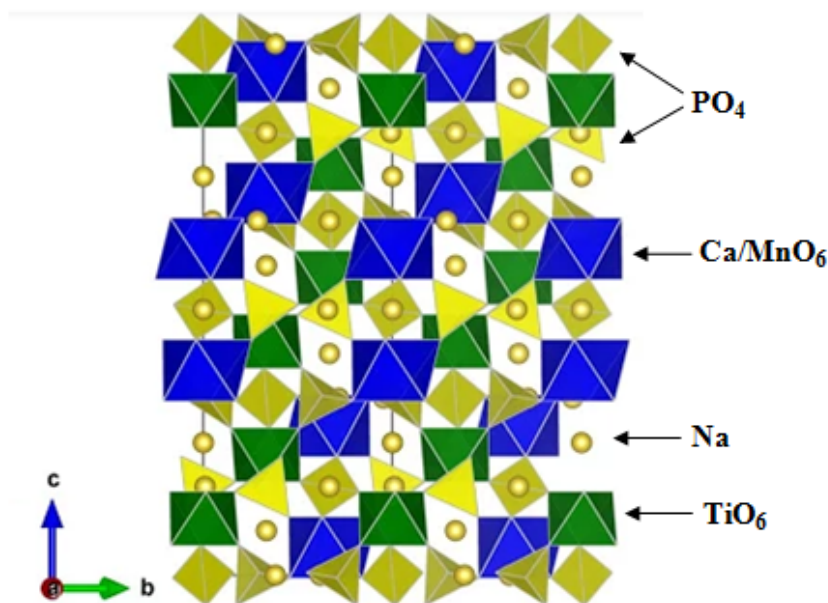
Figure 5: Structure of crystalline $Na_3Ca_{(1-x)}Mn_xTi(PO_4)_3$ ($x = 0, 1$) compounds.

3.5. EPR spectroscopy

Figure 6 presents the EPR spectra of $Na_3Ca_{1-x}Mn_xTi(PO_4)_3$ ($0 \leq x \leq 1$) glasses. All spectra show a strong signal centered at $g = 2.0$. Spectra of glasses with low manganese concentrations ($x = 0.01$; 0.05) are characterized by a hyperfine structure (hfs) which consists of six multiplets centered at $g = 2.0$, with a hyperfine coupling constant $A = 90$ G. Additional weaker signals are observed at lower magnetic fields, $g = 3.3$ and $g = 4.3$, for the low concentrations ($x = 0.01$, 0.05, 0.25).
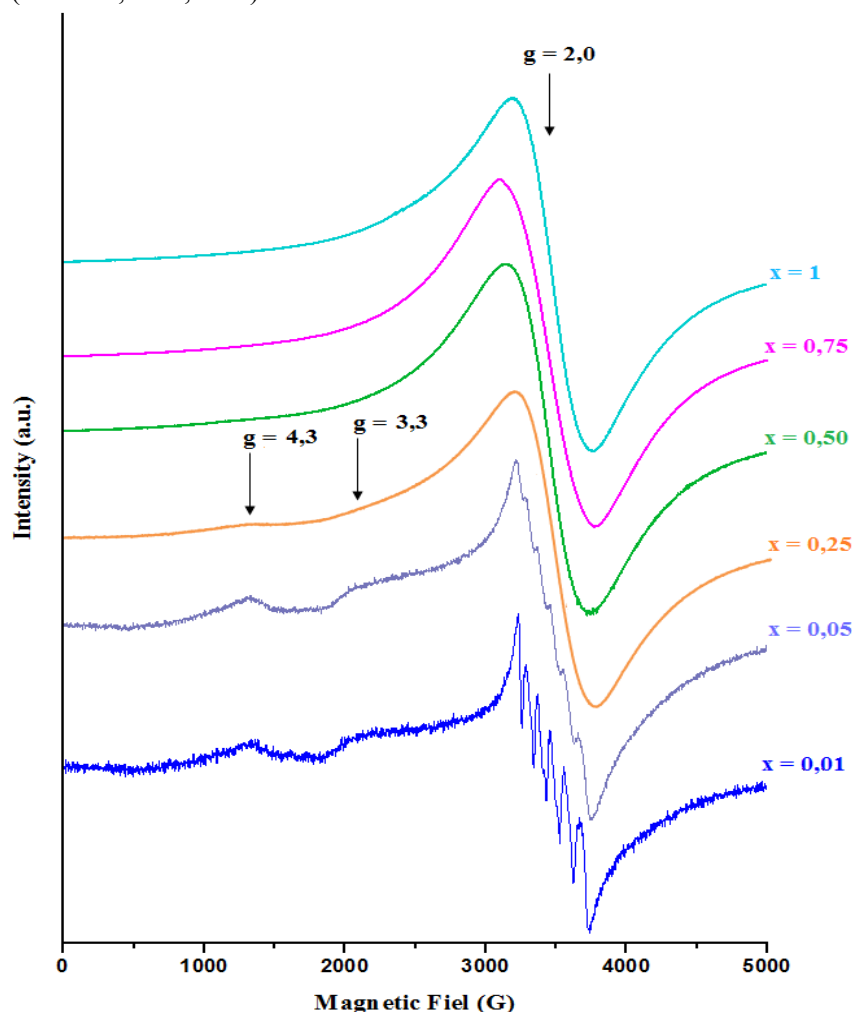

Figure 6: EPR spectra of $Na_3Ca_{1-x}Mn_xTi(PO_4)_3$ ($0 \leq x \leq 1$) glasses.

EPR of divalent manganese was investigated in a variety of glass system [44 - 46]. The d^5 electronic configuration of Mn^{2+} ion has a $^6S_{5/2}$ ground state in the free ion and possesses zero orbital angular momentum. The hyperfine splitting of $2I+1 = 6$ lines, arises from the interaction between the spin of the unpaired $3d^5$ electrons ($S = 5/2$) with the spin of the ^{55}Mn nucleus, $I(^{55}Mn, 100\%) = 5/2$. This isotropic signal at $g = 2.0$ is due to Mn^{2+} ions in an environment close to octahedral symmetry.

The hfs line-width increases with the MnO content, from $x = 0.01$ to $x = 0.05$, due to the increase of the dipolar interaction. The hyperfine structure disappears when MnO content increases ($x > 0.05$). The strongly distorted versions of the octahedral vicinity, subjected to strong crystal field effects, give rise to absorptions at $g = 4.3$ and 3.3. These absorptions are less intense than the one at $g = 2.0$ and appear only for low concentrations of manganese ($x = 0.01$, 0.05 and 0.25). There is a relatively small concentration of Mn^{2+} ions involved in such structural units. The same behavior in the low concentration range was observed for other glass systems [44, 46].

The structure of $Na_3Ca_{1-x}Mn_xTi(PO_4)_3$ ($0 \leq x \leq 1$) glasses shows an evolution from structural units involving Mn^{2+} ions in well-defined vicinities, to structural units containing clustered magnetic ions. The change of the shape of $g = 2.0$ EPR-spectra when the content of manganese ions increases revealed this evolution. The line intensities at $g = 4.3$ and 3.3 are small enough and indicate a relative low concentration of isolated Mn^{2+} ions involved in structural units strongly distorted of the octahedral vicinities.

3.6. Raman spectroscopy

Figure 7 shows the Raman spectra of $Na_3Ca_{1-x}Mn_xTi(PO_4)_3$ ($0 \leq x \leq 1$) glasses in the frequency region between 100 and 1800 cm^{-1}. Table 2 gives Raman wave-numbers and their assignments. Figure 8 represents the Raman spectra of the crystalline compounds $NaTi_2(PO_4)_3$, $LiTiO(PO_4)$ and $Cs_2MnP_2O_7$, which belong respectively to Nasicon (monophosphate), oxyphosphate, and diphosphate families. The crystalline structure of $NaTi_2(PO_4)_3$ [33] and $LiTiO(PO_4)$ [47 – 50] is based on a 3D framework built of TiO_6 octahedra and PO_4 tetrahedra sharing corners; this 3D framework has cavities where Na^+ and Li^+ ions are located. In both compounds, the PO_4 tetrahedra are isolated from each-other. The TiO_6 octahedra are rather regular and isolated from each-other in $NaTi_2(PO_4)_3$ (Ti-O distances : 1.90-2.00 Å), while in $LiTiO(PO_4)$ they are linked to each-other by corners to form -Ti-O-Ti-O-Ti-O- infinite chains with alternating short (1.70 Å) and long (2.28 Å) Ti-O bonds; these chains are connected by PO_4 tetrahedra. The structure of $Cs_2MnP_2O_7$ diphosphate contains P_2O_7 groups [51]. For $NaTi_2(PO_4)_3$, in which PO_4 tetrahedra, as well as TiO_6 octahedra, are isolated from each other, no peak is observed in 700–800 cm^{-1} region, in good agreement with previous Raman studies of iso-structural titanium phosphates [36, 37, 52]. In contrast, Raman spectra of titanyl oxyphosphates show a strong peak in this region, at 745 cm^{-1} for $NaTiOPO_4$ [53, 54], 783 cm^{-1} for $LiTiOPO_4$ [50], and ≈ 750 cm^{-1} for $M_{0.5}TiOPO_4$ (M=Mg, Co, Ni) [36, 55, 56]. This strong peak is associated with Ti-O bond. It can be attributed to synchronous vibrations of all Ti-O bonds of the -Ti-O-Ti-O-Ti- chains as previously reported by Bamberger et al. [53, 54]. The Raman spectrum of $Cs_2MnP_2O_7$ shows a strong and sharp peak at 1020 cm^{-1} and a strong one at 700 cm^{-1}, attributed respectively to asymmetric and symmetric stretching vibrations of P-O bonds in P-O-P bridge (ν_1 and ν_3 modes) [51].
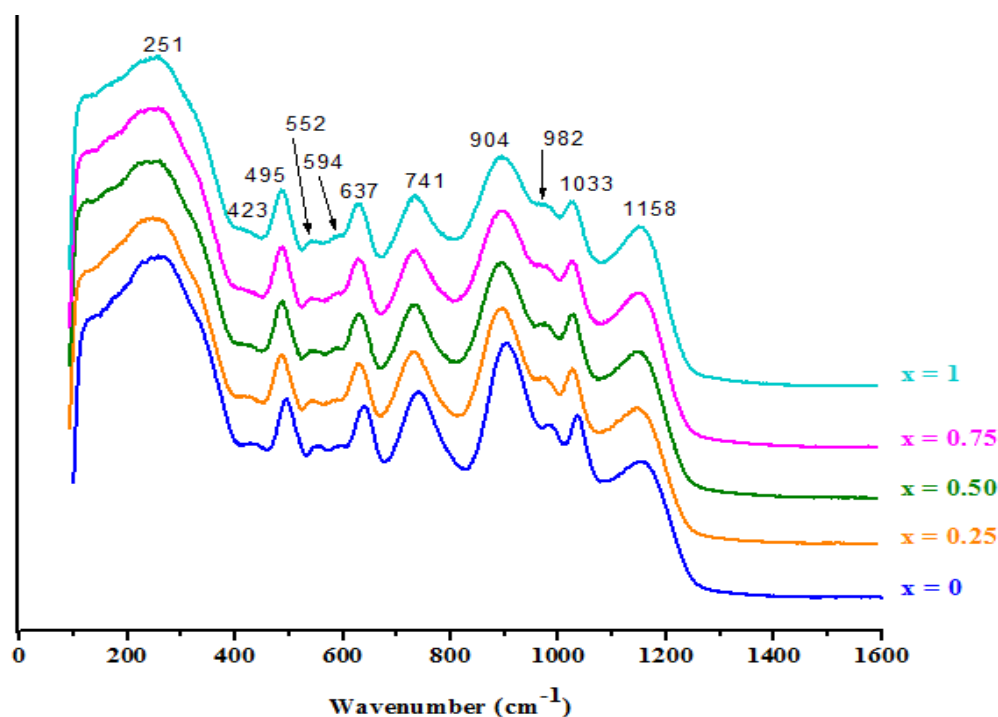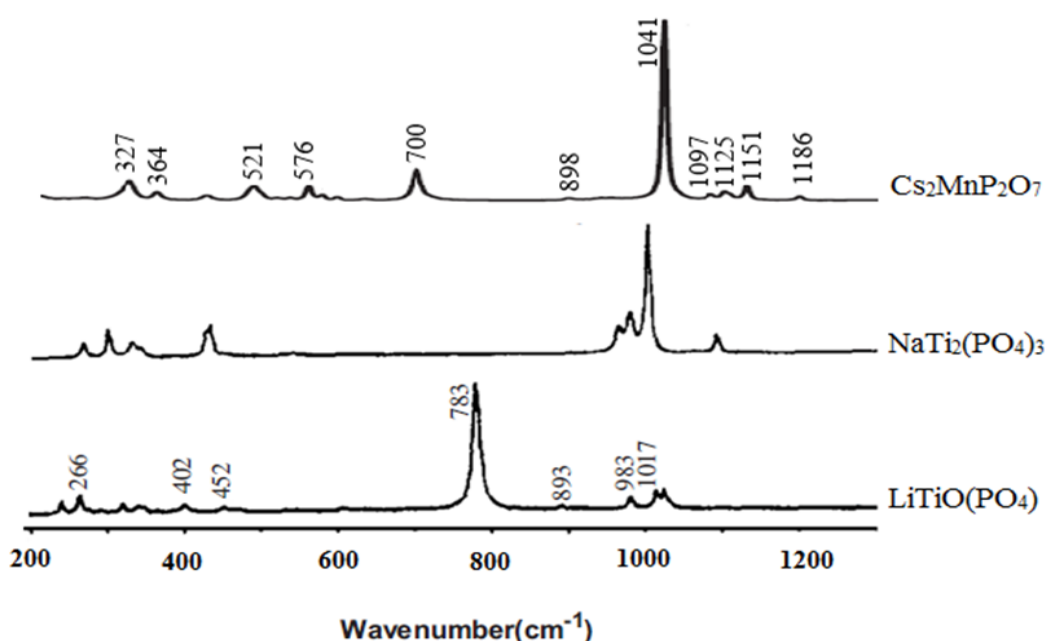

Figure 7: Raman spectra of $Na_3Ca_{1-x}Mn_xTi(PO_4)_3$ ($0 \leq x \leq 1$) glasses.

The peaks observed for $Na_3Ca_{1-x}Mn_xTi(PO_4)_3$ ($0 \leq x \leq 1$) glasses, in the high frequency region 830 – 1250 cm^{-1} are due to monophosphate (PO_4) and diphosphate (P_2O_7) groups. The peak at ~1033 cm^{-1}, relatively sharp, is due to $P_2O_7^{4-}$ diphosphate ions [51]. The strong peak at ~750 cm^{-1} is assigned to Ti-O vibrations in the -Ti-O-Ti-O- chains [50, 52 - 56], which indicates that the glass structure contains TiO_6 octahedra linked by corners and form short -Ti-O-Ti-O- chains. These chains are certainly linked to phosphate groups to form -Ti-O-P- linkages. The peaks observed between 400 and 640 cm^{-1} are attributed to O-P-O and P-O-P deformations (δ_2 and δ_4 PO_4 modes) and Ti-O vibrations of TiO_6 octahedra. The peaks observed below 300 cm^{-1} are attributed to lattice vibrations. As can be observed from Figure 7 and Table 2, no significant change is observed in the spectra, when manganese replaces calcium, indicating that Mn^{2+} ions don't modify significantly the glass structure and occupy the interstitial sites of the framework, in good agreement with glass transition temperature and molar volume variations. We can then conclude that Mn^{2+} and Ca^{2+} ions act as network modifiers in the glasses, unlike in the crystalline phases where they are part of the framework.

Table 2. Raman wave numbers (cm^{-1}) peak assignments of Na$_3$Ca$_{1-x}$Mn$_x$Ti(PO$_4$)$_3$ ($0 \leq x \leq 1$) glasses (w: weak, vw: very weak, m: medium, s: strong, vs: very strong).

x = 0	x = 0.25	x = 0.5	x = 0.75	x = 1	Assignment
1154 m	1155	1156	1158	1158	
1036 m	1033	1036	1034	1033	PO$_4$ + P$_2$O$_7$ (v_1 and v_3 modes)
985 w	984	984	984	982	
903 vs	903	904	903	904	
740 s	741	743	743	741	-Ti-O-Ti-O-Ti- chains + P-O-P
639 m/s	639	638	637	637	
590 vw	592	593	590	594	Ti-O vibrations of TiO$_6$ octahedra
553 vw	549	548	550	552	+
495 m/s	495	495	494	495	O-P-O and P-O-P deformations (δ modes)
430 vw	432	433	425	423	
256 vs	254	252	256	251	Lattice vibrations

Figure 8: Raman spectra of the crystalline compounds LiTiO(PO$_4$) [50], NaTi$_2$(PO$_4$)$_3$ [56] and Cs$_2$MnP$_2$O$_7$ [51].

4. Conclusion

Na$_3$Ca$_{1-x}$Mn$_x$Ti(PO$_4$)$_3$ ($0 \leq x \leq 1$) phosphates can be prepared in both crystalline and glassy forms. The crystalline materials belong to the Nasicon family. Their structure consists of a 3D network of PO$_4$ tetrahedra and AO$_6$ [A = Ti, Ca/Mn] octahedra sharing corners; Na$^+$ ions occupy interstitial sites. EPR study of glasses shows that Mn^{2+} ions occupy octahedral sites, with predominantly ionic character of the bonding between Mn^{2+} and O^{-2} ions. Raman spectroscopy study shows that the glasses contain PO$_4$ and P$_2$O$_7$ groups, and short -Ti-O-Ti-O-Ti- chains. The presence of these chains indicates that the TiO$_6$ octahedra are linked to each other through corners, unlike in the corresponding Nasicon crystalline phases where they are isolated and connected to each other via PO$_4$ tetrahedra. All results obtained for the glassy materials indicate that MnO and CaO oxides act as glass modifiers.

References

1. B. C. Sales and L. A. Boatner, *Science*. 226 (1984) 45–49.
2. D. E. Day, Z. Wu, C. S. Ray and P. Hrma, *J. Non-Cryst*. Solids. 241 (1998) 1–12.
3. A. K. Padhi, K. S. Nanjundaswamy and J. B. Goodenough, *J. Electrochem. Soc.* 144 (1997) 1188–1194.
4. N. Ravet, Y. Chouinard, J. F. Magnan, S. Besner, M. Gauthier and M. Armand, *J. Power Sources*. 97 (2001) 503–507.
5. C. Delmas, M. Maccario, L. Croguennec, F. Le Cras and F. Weill, *Nat. Mater*. 7 (2008) 665–671.
6. V. C. Seixas and O. A. Serra, *Molecules*. 19 (2014) 9907–9925.
7. M. Llusar, A. Zielinska, M. A. Tena, J. A. Badenes and G. Monrós, *J. Eur. Ceram. Soc.* 30 (2010) 1887–1896.
8. S. Laha, R. Sharma, S. V. Bhat, M. L. P. Reddy, J. Gopalakrishnan and S. Natarajan, *Bull. Mater. Sci.* 34 (2011) 1257–1262.
9. N. Gorodylova, V. Kosinová, Ž. Dohnalová, P. Bělina and P. Šulcová, *Dyes and Pigments*. 98 (2013) 393–404.
10. A. El Jazouli, B. Tbib, A. Demourgues and M. Gaudon, *Dyes and Pigments*. 104 (2014) 67–74.
11. H. Danielmeyer and H. Weber, IEEE J. *Quantum Electron*. 8 (1972) 805–808.
12. X.-J. Wang, D. Jia and W. M. Yen, *J. Lumin.* 102 (2003) 34–37.
13. J. H. Campbell and T. I. Suratwala, *J. Non-Cryst. Solids*. 263 (2000) 318–341.
14. Z. Hao, J. Zhang, X. Zhang, S. Lu, Y. Luo, X. Ren and X. Wang, *J. Lumin.* 128 (2008) 941–944.
15. D. K. Yim, H. J. Song, I.-S. Cho, J. S. Kim and K. S. Hong, *Mater. Lett.* 65 (2011) 1666–1668.
16. G. B. Nair and S. J. Dhoble, *Luminescence*. 32 (2017) 125–128.
17. J. C. Knowles, *J. Mater. Chem.* 13 (2003) 2395–2401.
18. R. Schnettler, J. P. Stahl, V. Alt, T. Pavlidis, E. Dingeldein and S. Wenisch, Eur. *J. Trauma*. 30 (2004) 219–229.
19. E. A. A. Neel, D. M. Pickup, S. P. Valappil, R. J. Newport and J. C. Knowles, *J. Mater. Chem.* 19 (2009) 690–701.
20. F. Chen, Y. Zhu, J. Wu, P. Huang and D. Cui, *Nano Biomed. Eng*. 4(1) (2012) 41-49.
21. Z. Wang, Z. Tang, F. Qing, Y. Hong and X. Zhang, *Nano*. 7 (2012) 1230004-12300046.
22. A. Kiani, N. J. Lakhkar, V. Salih, M. E. Smith, J. V. Hanna, R. J. Newport, D. M. Pickup and J. C. Knowles, *Phil. Trans. R. Soc. A*. 370 (2012) 1352–1375.
23. N. M. Shash, F. E. Salman, M. K. El-Mansy and H. A. Ghodair, *J. Phys. Chem. Solids*. 65 (2004) 891–900.
24. J. A. Wilder, *J. Non-Cryst. Solids*. 38 (1980) 879–884.
25. S. M. Hsu, S. W. Yung, R. K. Brow, W. L. Hsu, C. C. Lu, F. B. Wu and S. H. Ching, *Mater. Chem. Phys.* 123 (2010) 172–176.
26. M. Alami, A. Mouline, R. Brochu, R. Olazcuaga, C. Parent and G. Le Flem, *Mat. Res. Bull.* 35 (2000) 899–908.
27. R. O. Omrani, S. Krimi, J. J. Videau, I. Khattech, A. El Jazouli and M. Jemal, *J. Non-Cryst. Solids*. 389 (2014) 66–71.
28. W. Ahmina, M. El Moudane, M. Zriouil and M. Taibi, *J. Mater. Environ. Sci.* 8 (2017) 4193-4198.
29. R. K. Brow, *J. Non-Cryst. Solids*. 263 (2000) 1–28.
30. S. Krimi, A. El Jazouli, L. Rabardel, M. Couzi, I. Mansouri and G. Le Flem, *J. Solid State Chem.* 102 (1993) 400–407.
31. S. Krimi, I. Mansouri, A. El Jazouli, J. P. Chaminade, P. Gravereau and G. Le Flem, *J. Alloys Compd.* 188 (1992) 120–122.
32. S. Krimi, I. Mansouri, A. El Jazouli, J. P. Chaminade, P. Gravereau and G. Le Flem, *J. Solid State Chem*. 105 (1993) 561–566.
33. L.-O. Hagman, P. Kierkegaard, P. Karvonen, A. I. Virtanen and J. Paasivirta, *Acta Chem. Scand.* 22 (1968) 1822–1832.
34. J. B. Goodenough, H.-P. Hong and J. A. Kafalas, *Mater. Res. Bull.* 11 (1976) 203–220.
35. A. El Jazouli, Advanced Materials Research, *Trans Tech Publ.* 1 (1994) 105–114.
36. A. El Jazouli, S. Krimi, B. Manoun, J. P. Chaminade, P. Gravereau and D. De Waal, *Ann. Chim. Sci. Mater.* 23 (1998) 7–10.
37. S. Krimi, A. El Jazouli, A. Lachgar, L. Rabardel, D. de Waal and J. R. Ramos-Barrado, *Ann. Chim. Sci. Mater.* 25 (2000) S75-S78.
38. Saida Kaoua, Thesis. *University Hassan II, Casablanca.* (2010).
39. S. Krimi, A. El Jazouli and A. Lachgar, *Acta Crystallogr. A*. 63 (2007) 291–292.

40. H. Gao and J. B. Goodenough, *Angew. Chem.* 128 (2016) 12960–12964.
41. H. Gao, Y. Li, K. Park and J. B. Goodenough, *Chem. Mater.* 28 (2016) 6553–6559.
42. M. B. Volf, "Mathematical Approach to Glass"*, Glass Science and Technology, Ed Elsevier, Amsterdeem.* 9 (1988).
43. W. Ahmina, M. El Moudane, M. Zriouil and M. Taibi, *J. Mater. Environ. Sci.* 7 (3) (2016) 694-699.
44. I. Ardelean, M. Peteanu, O. Cozar, V. Simon, V. Mih and G. Botezan, *J. Mater. Sci. Technol.* 15 (1999) 453–456.
45. D. Toloman, L. M. Giurgiu and I. Ardelean, *Phys. B Condens. Matter.* 404 (2009) 4198–4201.
46. D. Möncke, E. I. Kamitsos, A. Herrmann, D. Ehrt and M. Friedrich, *J. Non-Cryst. Solids.* 357 (2011) 2542–2551.
47. P.G. Nagornoy, A.A. Kapshuck, N.V. Stus, N.S. Slobodyanik and A.N. Chernega, *Russ J. Inorg Chem.* 36 (1991) 1551.
48. A. Robertson, J. G. Fletcher, J. M. S. Skakle and A. R. West, *J. Solid State Chem.* 109 (1994) 53–59.
49. B. Manoun, A. El Jazouli, P. Gravereau and J.-P. Chaminade, *Mater. Res. Bull.* 40 (2005) 229–238.
50. M. Chakir, A. El Jazouli, J.-P. Chaminade, F. Bourée and D. De Waal, *J. Solid State Chem.* 179 (2006) 18–28.
51. S. Kaoua, S. Krimi, S. Péchev, P. Gravereau, J.-P. Chaminade, M. Couzi and A. El Jazouli, *J. Solid State Chem.* 198 (2013) 379–385.
52. S. Krimi, A. El Jazouli, D. de Waal and J.R. Ramos-Barrado, *Proceedings of the sixth Conference of the European Society of Glass Science and Technology (Glass Odissey), Ed Université Montpellier II*, Montpelier. (2002).
53. C. E. Bamberger and G. M. Begun, *J. Common Met.* 134 (1987) 201–206.
54. C. E. Bamberger, G. M. Begun and O. B. Cavin, *J. Solid State Chem.* 73 (1988) 317–324.
55. H. Belmal, *Thesis, University Hassan II Casablanca.* (2003).
56. S. Benmokhtar, A. El Jazouli, S. Krimi, J.-P. Chaminade, P. Gravereau, M. Ménétrier and D. De Waal, *Mater. Res. Bull.* 42 (2007) 892–903.

(2018) ; http://www.jmaterenvironsci.com